Cellular and Molecular Biology

Journal homepage: www.cellmolbiol.org

Emetine and Indirubin- 3- monoxime interaction with human brain acetylcholinesterase: A computational and statistical analysis

Syed Sayeed Ahmad[1], Haroon Khan[2]*, Mohammad Khalid [3], Abdulraheem SA Almalki[4]

[1]*Department of Bioengineering, Faculty of Engineering, Integral University, Lucknow-226026, India; (S.S)*
[2]*Department of Pharmacy, Abdul Wali Khan University, Mardan-23200, Pakistan; (H.K.)*
[3]*College of Pharmacy, Department of Pharmacognosy, Prince Sattam Bin Abdul Aziz University, Alkharj 16278, Riyadh, Saudi Arabia.*
[4]*Department of Chemistry, Faculty of Science, Taif University, Taif 21974, Saudi Arabia*

ARTICLE INFO

Original paper

Article history:
Received: September 10, 2021
Accepted: November 06, 2021
Published: December 01, 2021

Keywords:
Emetine; Indirubin- 3-monoxime; Alzheimer's disease; binding energy; inhibition constant; statistical analysis

ABSTRACT

Alzheimer's disease is a chronic neurodegenerative ailment and the most familiar type of dementia in the older population with no effective cure to date. It is characterized by a decrease in memory, associated with the mutilation of cholinergic neurotransmission. Presently, acetylcholinesterase inhibitors have emerged as the most endorsed pharmacological medications for the symptomatic treatment of mild to moderate Alzheimer's disease. This study aimed to research the molecular enzymatic inhibition of human brain acetylcholinesterase by a natural compound emetine and I3M. Molecular docking studies were used to identify superior interaction between enzyme acetylcholinesterase and ligands. Furthermore, the docked acetylcholinesterase-emetine complex was validated statistically using an analysis of variance in all tested conformers. In this interaction, H-bond, hydrophobic interaction, pi-pi, and Cation-pi interactions played a vital function in predicting the accurate conformation of the ligand that binds with the active site of acetylcholinesterase. The conformer with the lowest free energy of binding was further analyzed. The binding energy for acetylcholinesterase complex with emetine and I3M was -9.72kcal/mol and -7.09kcal/mol, respectively. In the current study, the prediction was studied to establish a relationship between binding energy and intermolecular energy (coefficient of determination [R2 linear = 0.999), and intermolecular energy and Van der wall forces (R2 linear = 0.994). These results would be useful in gaining structural insight for designing novel lead compounds against acetylcholinesterase for the effective management of Alzheimer's disease.

DOI: http://dx.doi.org/10.14715/cmb/2021.67.4.12

Introduction

Neurological disorders (ND) are one of the first reasons for death, especially in a developed nation and Alzheimer's disease (AD) is at the top of the list (1). AD is a dynamic and irreversible ND and the most widely recognized foundation of dementia in the older population > 60 years and the seventh leading cause of death throughout the world (2, 3). In the US alone, an increasing number of individuals are being diagnosed with AD. Statistics released data by the 2018 AD, details, and statistics report indicates that AD financial records for approximately 60-70% of all types of dementia cases and 5.5 million individuals of varying ages in the US have been evaluated to have AD. Additionally, this report indicates that around 47.5 million individuals worldwide are living with dementia actuated by this disease and it is evaluated that by 2050, over 115 million individuals will have dementia (4, 5).

In AD brains, the cholinergic network is the most drastically affected, demonstrating restoration of acetylcholine (ACh) and different markers of cholinergic activity (6). In light of this perception, the medications galantamine (7), donepezil (8), and rivastigmine (9) have been affirmed by the US Food and Drug Administration (FDA) and presently promoted for the symptomatic treatment of AD (10). Cholinesterase is a family of enzymes that catalyze the neurotransmitter ACh through hydrolysis into choline and acetic acid. In AD, acetylcholinesterase (AChE) inhibitors act by preventing ACh breakdown, which is the basis of their use in treating this disease. The mechanism of action of most FDA-approved drugs for AD, which is based on the cholinergic

*Corresponding author. E-mail: haroonkhan@awkum.edu.pk

hypothesis, involves the enhancement of ACh levels in the diseased brain. Therefore, inhibition of AChE plays a significant role in enhancing cholinergic transmission in the diseased brain (11, 12). AChE is found in high concentrations principally in the red blood cells in addition to the brain at neuromuscular junctions and cholinergic synapses (13). Currently, cholinesterase inhibitors have been proven to be the most effective treatment for AD owing to their ability to affect cognition and function in AD (14). Experimental evidence indicates that general cholinesterase inhibitors targeting AChE have potential remedial advantages in the treatment of AD and other related dementia. Cholinesterase inhibitors improve cholinergic action by restraining AChE that hydrolyze ACh following synaptic discharge and, hence, prolongs the activity of ACh (15, 16).

Emetine is an alkaloid obtained from ipecac species that act as a blocking agent in the early S phase of DNA replication (17). It is a ribosomal and mitochondrial protein combination inhibitor, which hinders the synthesis of DNA and RNA. Emetine ties to the 40S ribosomal subunit to hinder the protein blend (18). Structure-movement relationship (SAR) contemplates have demonstrated that the N-2′position of emetine is pivotal to its hindrance to protein synthesis and must be an optional amine (19, 20). It was reported to be one of the most potent inducers of PPARG coactivator 1 (PGC)-1α expression. Increasing PGC-1α movement has been proposed to help control muscular dystrophy, diabetes, and ND (21, 22). It was additionally appeared to be an antagonist of dopamine (D1 and D3) receptors, substance P, and neurokinin NK3 (23).

Indirubin-3′-monoxime (I3M) is nontoxic with a low molecular weight compound having CDK inhibitor activity, with good solubility [40-42]. The compound was found to suppress tau phosphorylation in Sf9 cells expressing human tau 23 (43) and, in cerebellar granular neurons, it reduced apoptosis initiated by the withdrawal of potassium (44-46).

In this study, we elucidated the molecular enzymatic inhibition of human brain AChE by emetine and I3M using a state-of-the-art molecular docking approach. Based on the better free energy of binding emetine was well elaborated in this study and further analyzed by statistical analysis using an analysis of variance (ANOVA) of all conformers used with validation of the findings.

Materials and methods

Preparation of Receptor

The recombinant structure of human AChE was taken from the Research Collaboratory for Structural Bioinformatics (RCSB) Protein Data Bank (PDB, ID: 3LII) (http://www.rcsb.org/pdb/home/home.do). RCSB is a solitary, worldwide archive for data about the 3D structures of macromolecules, as determined by X-ray crystallography, NMR spectroscopy, and cryoelectron microscopy (24). The PDB record was cleaned and the heteroatoms of the receptor were removed since these are non-standard stores of the protein.

Preparation of Ligand and Lipinski's Rule of Five

The canonical Simplified Molecular Input Line Entry Specification (SMILES) details of the emetine and I3M were obtained from the PubChem database (http://www.ncbi.nlm.nih.gov/pccompound). The 3D structure was built using the online exhibition of CORINA (http://www.molecular-networks.com/products/corina). To check the properties of selected ligands like hydrogen donor/ acceptors, LogP, and molecular weight, Lipinski's rule of five was used (24).

ADMET Prediction

Pre-ADMET software was used for the investigation of solubility, plasma protein binding ability, intestinal absorption, blood-brain-barrier (BBB) penetration. Leads can be recognized by utilizing high-throughput screening approaches. To diminish the cost and clinical inefficacy of new medications, the compound dataset is adequately screened in the early stages for ADMET, since the available technologies for their assessment are advancing and becoming more sophisticated and reliable than previous methods are. These criteria all have an expected effect on the pharmacological and pharmacokinetic properties of drugs (25, 26).

Docking Simulations and Interaction Study

Polar H-atoms, Kollman joined particle, and atom compose parameters were included in the analysis, furthermore, non-polar H-atoms were merged in the

protein pdbqt. In the ligand pdbqt record, polar H-atoms were included, non-polar H-atoms were joined, and the number of torsions and rotatable bonds was portrayed. A cubic volume of 60 × 60 × 60 $Å^3$ with 0.408 Å grid point spacing and center axes coordinates as X: 90.81, Y: 83.98, and Z: -8.04 were set to cover the whole active site and enable ligands to move uninhibitedly [27]. The Lamarckian genetic algorithm was used for the receptor and ligand-flexible docking calculations. The conformer with the lowest ΔG was selected for further examination (28, 29).

Statistical Analysis

The SPSS version-20 was utilized to establish the relationship among the analyzed data.

Results and discussion

Identification of phenolic compounds through HPLC-UV technique

Results and discussion

The 3D structure of AChE empowers with two hemispheres that sandwich the synergist focus between the acyl-and omega-circles. These circles are considered as sidewalls of the active site gorge that is around 300 $Å^3$. The selected ligand was docked at the catalytic site where the quaternary ammonium of the choline of ACh interacted (30). It has been reported that cholinergic neurotransmitter levels are significantly reduced under conditions such as AD (31, 32), AChE is typically targeted in terms of enzyme inhibition since this strategy temporarily increases ACh levels. The thought that cholinergic shortfalls are centrally connected with the pathogenesis of neurodegenerative conditions, for example, AD particularly centers around the loss of cholinergic neurons and the following decrease of synapse levels (33).

In our study, data using PreADMET showed that human intestinal absorption of emetine and I3M was 96.595% and 88.66% respectively, which suggests that it is well absorbed through the intestine. Further, we found that emetine and I3M were moderately permeable since the absorption value through Caco-2 cells was 56.697 and 19.99 respectively. Subsequently, the plasma protein binding and BBB penetrability for emetine were 63.098 and 0.8754, while for I3M it was 99.81 and 4.79 respectively. The docking simulation system was performed using the AutoDock 4.2 program with a natural plant-derived compound. The compound was docked into the active site of the chosen target. The lowest energy of the docked conformation of the best group was chosen for further evaluation. It merits referencing that the ligands and protein side chains were held versatile by the docking programming all through the examination.

In the present examination, the active site of human brain AChE was found to cooperate with emetine through the 10 amino acid residues: Asp74, Trp86, Tyr124, Tyr133, Ser203, Phe295, Phe297, Tyr337, Phe338, and His447 (Figure 1). The free energy of binding (ΔG) and estimated inhibition constant (Ki) for the emetine-AChE complex interaction were -9.72kcal/mol and 75.07nM, respectively. The vital role of two H- bonds was established for the precise placing of the ligand, UNK1:H63-Tyr124:OH and Tyr133:HH-UNK1:O34 in the active site of AChE, with H- bond distances of 2.03938 and 2.16778 Å, respectively. Furthermore, the OH molecule of Tyr124 and HH group of Tyr133were found to interact with H63 and O34 of the ligand, respectively. Seven carbon atoms of ligand, C3, C13, C24, C25, C26, C27, and C28 were observed to be engaged with hydrophobic collaborations with amino acid deposits of the compound in which C3, C13, C24, C25, and C28 interacted with Trp86 and while C26 and C27 were attached to Phe297 and Phe295, respectively.

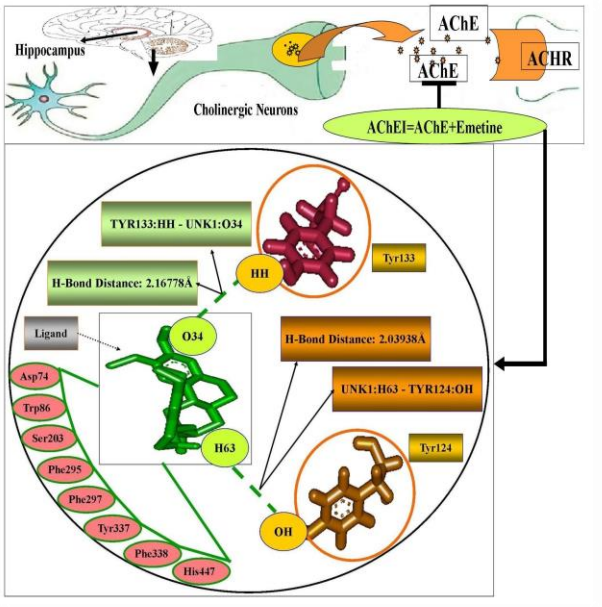

Figure 1. Structure of emetine and acetylcholinesterase (AChE) complex. Emetine is shown as a green stick.

In particular, one oxygen atom of the ligand, O3, formed a polar bond that included one amino acid residue Asp74 of the AChE enzyme. Cation pi-interactions were additionally observed in this interaction in which atoms O4, C28, and C29 interacted with Asp74 while atoms O3, C24, and C25 interacted with Asp86. Atoms such as C3 and C4 were observed to connect with the Tyr133 of the enzyme. In the Pi-Pi interaction, H29 and H30 of the selected ligand were associated with the Tyr337 and His447 residues of the enzyme. The entire interacting surface area for the generated complex was 873.79 $Å^2$. Van der Waals, hydrogen bonds, and desolvation energy components collectively contributed –10.22 kcal/mol for this interaction. The electrostatic energy component was -1.59 kcal/mol in this interaction. The total internal energy and intermolecular energies were -1.25 and -11.81 kcal/mol for the complex of the emetine and AChE, respectively. The findings of this interacting complex are summarized in Table1.

I3M was found to interact with AChE through 20 amino acid-like, Gln71, Tyr72, Asp74, Trp86, Asn87, Gly120, Gly121, Gly122, Tyr124, Ser125, Gly126, Tyr133, Glu202, Ser203, Phe297, Tyr337, Phe338, His447, Gly448, and Ile451. ΔG and Ki for the I3M-AChE complex were found to be -7.09kcal/mol and 6.49 µM, respectively. Two H- bonds were established in this interaction, TRP86:NE1 - :UNK1:O10 and TYR337:OH - :UNK1:O10 in the active site of AChE, with H- bond distances of 3.1877and 2.98454, respectively. The donor atom NE1 of Trp86 was found to interact with the O10 of I3M, while OH of Tyr337 was found to interact with O10 of I3M.

Van der Waals, hydrogen bonds, and desolvation energy components collectively contributed –7.56 kcal/mol for this interaction. The electrostatic energy component was -0.08 kcal/mol in this interaction. The intermolecular energy was -7.64 kcal/mol for the complex of the I3M and enzyme, respectively.

The binding affinity of emetine and I3M with AChE was found near about to different reported compounds like sargachromanol-I (-8.6kcal/mol), sargachromanol-G (-7.9kcal/mol) and dihydroberberine (-8.2 kcal/mol) (47).

Table 1. Interacting parameters of emetine with AChE

Sr. No.	Parameters	Outcomes
1.	H-bond	UNK1:H63-Tyr124 and Tyr133:HH-UNK1
2.	Polar bond	UNK1:O3-Asp74
3.	Hydrophobic interaction	UNK1:(C3, C13, C24, C25, C28)-Trp86
4.	Pi-Pi interaction	UNK1:H29-Tyr337 and UNK1:(H29, H30)-His447
5	Cation-Pi interaction	UNK1:(C3,C4)-Tyr133,UNK1:(O4,C28,C29)-Asp74 and UNK1:(O3, C24, C25)-Asp86
6.	Total interacting amino acid	Asp74, Trp86, Tyr124, Tyr133, Ser203, Phe295, Phe297, Tyr337, Phe338 and His447
7.	Free energy of binding (ΔG)	-9.72 kcal/mol
8.	Inhibition constant	75.07 nM
9.	Inter molecular energy	-11.81 kcal/mol
10.	Van der Waals, hydrogen bond and desolvation energy	-10.22 kcal/mol
11.	Electrostatic energy	-1.59 kcal/mol
12.	Total internal energy	-1.25 kcal/mol
13.	Interacting surface area	873.79 $Å^2$

Thermodynamics Analysis

For a better understanding of the sub-atomic recognition between a protein and its ligand, it is important to comprehend the physicochemical components underlying the protein-ligand interaction. In this section, the fundamental thermodynamics, interaction for ligand-protein binding, binding driving forces, and enthalpy-entropy compensation (34) are presented. The possibility of a protein-ligand association is constrained by the negative ΔG, which can be considered to decide the dependability of any protein-ligand complex or the coupling affinity of a ligand to a particular acceptor. It should be noticed that the free energy is a component of the condition of a framework and ΔG is portrayed by the underlying and last thermodynamic states (35, 36). The standard ΔG, which alludes to the free energy change assessed under 1 atm. pressure, at a temperature of 298 K, and the incredible reactant (protein and ligand) with 1 M, is identified with the binding consistent Kb by the Gibbs relationship as shown in the following equation:

$$\Delta G^o = -RT \ln Kb \qquad [1]$$

Where R is the gas constant (1.987 cal·K^{-1}·mol^{-1}) and temperature (T) in Kelvin. The ΔG at any time during the involvement is calculated as:

$$\Delta G = \Delta G^{o} + RT \ln Q \quad [2]$$

Where, Q is the reaction quotient, which is characterized as the extent of the grouping of the protein-ligand complex to the result of the centralizations of the free protein and free ligand at any minute in time. ΔG can be characterized as its enthalpy and entropic through the resulting condition:

$$\Delta G = \Delta H - T\Delta S \quad [3]$$

Where ΔH and ΔS are changing in enthalpy and entropy of the framework following ligand binding, respectively and T is the temperature in Kelvin.
Enthalpy is the proportion of the aggregate energy of a thermodynamic system and it is negative for exothermic conditions (37, 38). The value of the partition function (Q) for the complexes emetine and I3M with AChE was found to be the same as 10.08. The values of the free and internal energy for the target with emetine complex were -1369.20 and -5.00 kcal/mol, while for I3M with the target was -1371.31 and -7.07 kcal/mol respectively. The predicted value of entropy for both ligands with target has been found 4.58 kcal·mol^{-1}·K^{-1}. However, if enthalpy (-ΔH) and entropy (ΔS) are considered for the complex, the major contribution to free energy (-ΔG) comes from entropy (ΔS or -TΔS). The increase in entropy (i.e., positive value) indicated that the interaction was entropy-driven and the complex consisted of dominant hydrophobic interactions (39). All the above data were acquired at a temperature of 298.15 K.

Statistical Analysis

In this study, R^2= 1, indicating that 100% of the variation in the intermolecular energy was due to van der Waals forces and electrostatic energy as shown in Table 2. The functional relationship between the dependent and independent variables was identified as the relationship shown in Table 3.

Table 2. Model summary[b] of the dependent variable

Model	R	R^2	Adjusted R^2	SE of the estimate
1	1.000[a]	1.000	1.000	0.02538

[a]Predictors: (constant), van der Waals, and electrostatic energy and dependent variable: intermolecular energy.

Table 3. Coefficient[a] analysis between van der Waals force and electrostatic energy

Model		Unstandardized Coefficients		Standardized Coefficients	*t*	Sig.
		B	Std. Error	Beta		
1	(Constant)	0.025	0.083		0.301	0.772
	electrostatic energy	1.017	0.043	0.087	23.430	0.000
	van der Waals	1.001	0.004	1.034	278.845	0.000

[a] Dependent variable: intermolecular energy

The given expression was obtained to establish a relation between intermolecular energy, electrostatic energy, and van der Waal energy.

Inter molecular energy = 0.025 + 1.017 (electrostatic energy) + 1.001 ('Van der Waals' energy) (4)

An ANOVA was performed to determine whether the regression line was significant and the constructed relationship model was significant as shown in Table 4.

Table 4. Analysis of variance (ANOVA)[a] of the data

Model		Sum of Squares	df	Mean Square	*F*	Sig.
1	Regression	57.375	2	28.687	44528.767	0.000[b]
	Residual	0.005	7	0.001		
	Total	57.379	9			

[a]Dependent Variable: intermolecular energy & b. Predictors: (Constant), Van der Waals and electrostatic energy

The graphical representation of intermolecular energy and binding energy is shown in Figure 2.

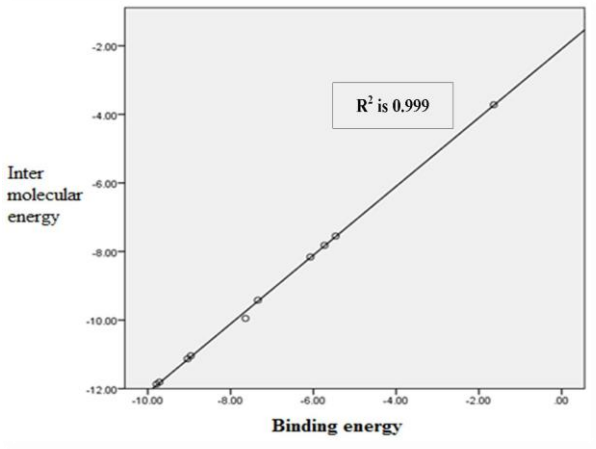

Figure 2. Relationship between intermolecular energy and binding energy.

The calculated R^2= 0.999, which indicated a linear relationship. The binding energy and intermolecular energy were plotted on the X and Y axes, respectively. The relationship between van der Waals forces and intermolecular energy was similarly linear with an R^2= 0.994, shown in Figure 3.

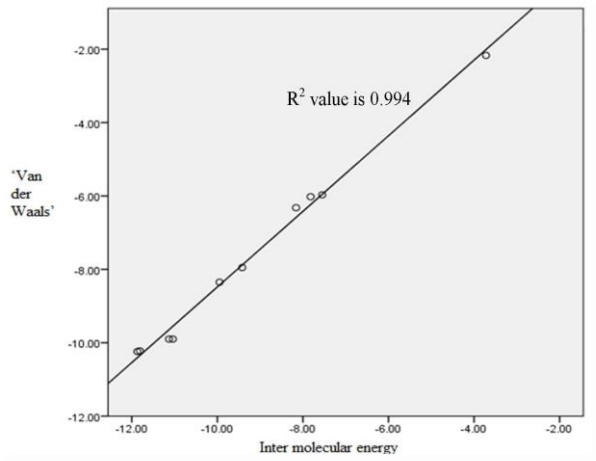

Figure 3. Relationship between van der Waal force and intermolecular energy.

The value of intermolecular energy and Van der Waals force was taken on X and Y-axis respectively. The final relationship between all the related energy Van der Waals, intermolecular energy, and electrostatic energy was shown in Figure 4.

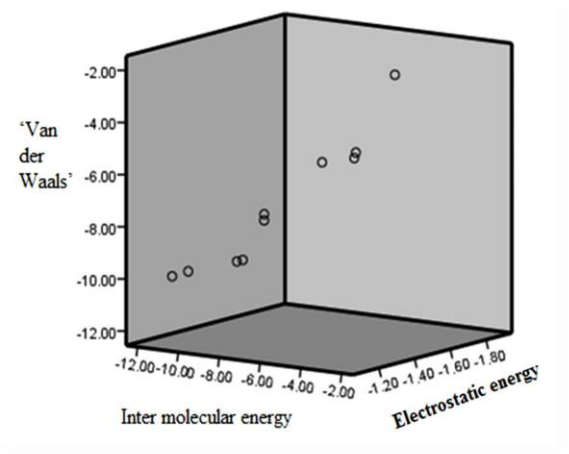

Figure 4. Relationship between van der Waal, intermolecular energy, and electrostatic energy.

Conclusions

This study examines the effective molecular interaction of the enzyme AChE with the emetine and I3M. The value of ΔG for emetine and I3M was -9.72 and -7.09 kcal/mol, respectively, while the remaining contribution to the free energy was entropy since the entropy was shown to increase during the interaction. Hence, we established that the interaction was entropy-driven with a prevalent hydrophobic interaction. This binding affinity was shown by the formation of different bonds such as H-bonds, polar bonds, cation-pi, Pi-Pi interactions, and hydrophobic interactions. Presently, the docked complex was validated statistically using an ANOVA for all the conformers used. This study confirmed that the ligand may prove to be a promising inhibitor of AChE for the management of AD. The scope of subsequent studies would focus on corroborating the 3D structure of the depicted complexes using X-ray crystallography to confirm the present findings.

Author Contributions

Conceptualization, S.S. and H.K.; methodology, S.S. and Q.R.; software, S.S.; validation, H.K.; formal analysis, H.K.; investigation, S.S.; resources, H.K.; data curation, S.S. and M.K.; writing—original draft preparation, S.S.; writing—review and editing, S.S.; M.K.; H.K., G.A. and L.R.; visualization, G.A. and L.R.; supervision, H.K. and L.R.; project administration, H.K. and L.R.; funding acquisition, H.K. All authors have read and agreed to the published version of the manuscript.

Conflicts of Interest

The authors declare no conflict of interest.

Acknowledgement

Taif University Researchers Supporting Project number (TURSP-2020/44), Taif University, Taif, Saudi Arabia

References

1. Ahmad SS, Akhtar S, Danish Rizvi SM, Kamal MA, Sayeed U, Khan M, Kalim A, Siddiqui M, Arif JM. Screening and elucidation of selected natural compounds for anti-Alzheimer's potential targeting BACE-1 enzyme: a case computational study. Curr Comput Aided Drug Design 2017; 13: 311-8.

2. Ahmad SS, Akhtar S, Jamal QM, Rizvi SM, Kamal MA, Khan MK, Siddiqui MH. Multiple Targets for the Management of Alzheimer's Disease. CNS Neurol Disord Drug Targets 2016; 15: 1279-9

3. Khan MB, Palaka BK, Sapam TD, Subbarao N, Ampasala DR. Screening and analysis of acetyl-cholinesterase (AChE) inhibitors in the context of Alzheimer's disease. Bioinformation 2018; 14: 414-8.

4. Association As. 2018 Alzheimer's disease facts and figures. Alzheimer's & Dementia volume 14, 2018; 367-9

5. Benson R. Psychological stress as a cause of lithium prophylaxis failure, a report of three cases. Dis Nerv Syst 1976; 37: 699-700.

6. Terry AV, Buccafusco JJ. The cholinergic hypothesis of age and Alzheimer's disease-related cognitive deficits: recent challenges and their implications for novel drug development. J Pharmacol Experi Ther 2003; 306: 821-7.

7. Richarz U, Gaudig M, Rettig K, Schauble B. Galantamine treatment in outpatients with mild Alzheimer's disease. Acta Neurologica Scandinavica 2014; 129: 382-2.

8. Birks JS, Harvey RJ. Donepezil for dementia due to Alzheimer's disease. Cochrane Database of systematic reviews 2018.

9. Birks JS, Evans JG. Rivastigmine for Alzheimer's disease. Cochrane Database of systematic reviews 2015

10. Rizzo S, Tarozzi A, Bartolini M, Da Costa G, Bisi A, Gobbi S, Belluti F, Ligresti A, Allarà M, Monti J-P. 2-Arylbenzofuran-based molecules as multipotent Alzheimer's disease modifying agents. Eur J Med Chem 2012; 58: 519-2

11. Colovic MB, Krstic DZ, Lazarevic-Pasti TD, Bondzic AM, Vasic VM. Acetylcholinesterase inhibitors: pharmacology and toxicology. Curr Neuropharmacol. 2013; 11: 315-5

12. Francis PT, Palmer AM, Snape M, Wilcock GK. The cholinergic hypothesis of Alzheimer's disease: a review of progress. J Neurol Neurosur Psychiat 1999; 66: 137-7.

13. Mushtaq G, H Greig N, A Khan J, A Kamal M. Status of acetylcholinesterase and butyrylcholinesterase in Alzheimer's disease and type 2 diabetes mellitus. CNS & Neurological Disorders-Drug Targets (Formerly Current Drug Targets-CNS & Neurological Disorders) 2014; 13: 1432-9.

14. Cummings JL. The role of cholinergic agents in the management of behavioural disturbances in Alzheimer's disease. Int J Neuropsychopharmacol 2000; 3: S21-S9.

15. Shaikh S, Verma A, Siddiqui S, S Ahmad S, MD Rizvi S, Shakil S, Biswas D, Singh D, H Siddiqui M, Shakil S. Current acetylcholinesterase-inhibitors: A neuroinformatics perspective. CNS & Neurol Disord Drug Target. 2014; 13: 391-1.

16. Kamal M, Al-Jafari A, Greig N. Interaction of new anti-alzheimer's disease agents with cholinesterase: P. 274. J Neurochem. 2005; 94.

17. Akinboye ES, Bakare O. Biological activities of emetine. The Open Natural Products Journal 2011; 4.

18. Akinboye ES, Rosen MD, Bakare O, Denmeade SR. Anticancer activities of emetine prodrugs that are proteolytically activated by the prostate specific antigen (PSA) and evaluation of in vivo toxicity of emetine derivatives. Bioorg Med Chem. 2017; 25: 6707-7.

19. Grollman AP. Structural basis for inhibition of protein synthesis by emetine and cycloheximide based on an analogy between ipecac alkaloids and glutarimide antibiotics. Proceedings of the National Academy of Sciences of the United States of America 1966; 56: 1867

20. Troconis M, Ma W, Nichols DE, McLaughlin J. Molecular modeling study of tubulosine and other related ipecac alkaloids. Journal of computer-aided molecular design 1998; 12: 411-418

21. Arany Z, Wagner BK, Ma Y, Chinsomboon J, Laznik D, Spiegelman BM. Gene expression-based

screening identifies microtubule inhibitors as inducers of PGC-1α and oxidative phosphorylation. Proceedings of the National Academy of Sciences 2008; 105: 4721-4726
22. Zhang Y, Ba Y, Liu C, Sun G, Ding L, Gao S, Hao J, Yu Z, Zhang J, Zen K. PGC-1α induces apoptosis in human epithelial ovarian cancer cells through a PPARγ-dependent pathway. Cell research 2007; 17: 363-373
23. Keiser MJ, Roth BL, Armbruster BN, Ernsberger P, Irwin JJ, Shoichet BK. Relating protein pharmacology by ligand chemistry. Nature biotechnology 2007; 25: 197-206
24. Berman HM, Westbrook J, Feng Z, Gilliland G, Bhat TN, Weissig H, Shindyalov IN, Bourne PE. The protein data bank. Nucleic acids research 2000; 28: 235-242
25. Hassan Baig M, Ahmad K, Roy S, Mohammad Ashraf J, Adil M, Haris Siddiqui M, Khan S, Amjad Kamal M, Provazník I, Choi I. Computer aided drug design: success and limitations. Current pharmaceutical design 2016; 22: 572-581
26. Selick HE, Beresford AP, Tarbit MH. The emerging importance of predictive ADME simulation in drug discovery. Drug Discovery Today 2002; 7: 109-116
27. Shaikh S, S Ahmad S, A Ansari M, Shakil S, MD Rizvi S, Shakil S, Tabrez S, Akhtar S, A Kamal M. Prediction of comparative inhibition efficiency for a novel natural ligand, Galangin against human brain Acetylcholinesterase, butyrylcholinesterase and 5-Lipoxygenase: a Neuroinformatics study. CNS & Neurological Disorders-Drug Targets (Formerly Current Drug Targets-CNS & Neurological Disorders) 2014; 13: 452-459
28. Rehman A, Akhtar S, Siddiqui MH, Sayeed U, Ahmad SS, Arif JM, Khan MK. Identification of potential leads against 4-hydroxytetrahydrodipicolinate synthase from Mycobacterium tuberculosis. Bioinformation 2016; 12: 400-407
29. Ahmad K, Khan S, Adil M, Saeed M, Srivastava AK. Structure based molecular inhibition of Caspase-8 for treatment of multi-neurodegenerative diseases using known natural compounds. Bioinformation 2014; 10: 191-5
30. Alam A, Shaikh S, S Ahmad S, A Ansari M, Shakil S, MD Rizvi S, Shakil S, Imran M, Haneef M, M Abuzenadah A. Molecular interaction of human brain acetylcholinesterase with a natural inhibitor Huperzine-B: An Enzoinformatics approach. CNS & Neurological Disorders-Drug Targets (Formerly Current Drug Targets-CNS & Neurological Disorders) 2014; 13: 487-490
31. Arendt T, Brückner MK, Lange M, Bigl V. Changes in acetylcholinesterase and butyrylcholinesterase in Alzheimer's disease resemble embryonic development—a study of molecular forms. Neurochemistry international 1992; 21: 381-396
32. Mufson EJ, Counts SE, Perez SE, Ginsberg SD. Cholinergic system during the progression of Alzheimer's disease: therapeutic implications. Expert review of neurotherapeutics 2008; 8: 1703-1718
33. Zimmermann M. Neuronal AChE splice variants and their non-hydrolytic functions: redefining a target of AChE inhibitors? British journal of pharmacology 2013; 170: 953-967
34. Du X, Li Y, Xia Y-L, Ai S-M, Liang J, Sang P, Ji X-L, Liu S-Q. Insights into protein–ligand interactions: mechanisms, models, and methods. International journal of molecular sciences 2016; 17: 144
35. Gilson MK, Zhou H-X. Calculation of protein-ligand binding affinities. Annu. Rev. Biophys. Biomol. Struct. 2007; 36: 21-42
36. Gibbs JW. A method of geometrical representation of the thermodynamic properties by means of surfaces. Transactions of Connecticut Academy of Arts and Sciences 1873: 382-404
37. Li H, Xie Y, Liu C, Liu S. Physicochemical bases for protein folding, dynamics, and protein-ligand binding. Science China Life Sciences 2014; 57: 287-302
38. Cooper A, Johnson CM. Introduction to microcalorimetry and biomolecular energetics. Microscopy, optical spectroscopy, and macroscopic techniques: Springer, 1994; 109-124
39. Khan M, Goswami U, Rojatkar S, Khan M. A serine protease inhibitor from hemolymph of green mussel, Perna viridis. Bioorganic & medicinal chemistry letters 2008; 18: 3963-3967.
40. Zahler S, Liebl J, Fürst R, Vollmar AM. Anti-angiogenic potential of small molecular inhibitors of cyclin dependent kinases in vitro. Angiogenesis 2010,13, 239–249

41. Liao XM, Leung KN. Indirubin-3'-oxime induces mitochondrial dysfunction and triggers growth inhibition and cell cycle arrest in human neuroblastoma cells. Oncol Rep 2013,29,371–379.
42. Shelton SB, Krishnamurthy P, Johnson GV. Effects of cyclin-dependent kinase-5 activity on apoptosis and tau phosphorylation in immortalized mouse brain cortical cells. J Neurosci Res 2004,76,110–120.
43. Leclerc S, Garnier M, Hoessel R, Marko D, Bibb JA, Snyder GL, Greengard P, Biernat J, Wu YZ, Mandelkow EM, Eisenbrand G, Meijer L. Indirubins inhibit glycogen synthase kinase-3 beta and CDK5/p25, two protein kinases involved in abnormal tau phosphorylation in Alzheimer's disease. A property common to most cyclin-dependent kinase inhibitors? J Biol Chem 2001,276,251–260.
44. Xie Y, Liu Y, Ma C, Yuan Z, Wang W, Zhu Z, Gao G, Liu X, Yuan H, Chen R, Huang S, Wang X, Zhu X, Wang X, Mao Z, Li M. Indirubin-3′-oxime inhibits c-Jun NH2-terminal kinase: anti-apoptotic effect in cerebellar granule neurons. Neurosci Lett 2004,367,355–359.
45. Fathi A., Barak M, Damandan M, Amani F, Moradpour R, Khalilova I., Valizadeh M. Neonatal Screening for Glucose-6-phosphate dehydrogenase Deficiency in Ardabil Province, Iran, 2018-2019. Cell Mol Biomed Rep 2021; 1(1): 1-6.
46.. Kazemi E, Zargooshi J, Kaboudi M, Heidari P, Kahrizi D, Mahaki B, Mohammadian Y, Khazaei H, Ahmed K. A genome-wide association study to identify candidate genes for erectile dysfunction. Brief Bioinforma 2021;22(4):bbaa338. https://doi.org/10.1093/bib/bbaa338
47. Lee JP, Kang MG, Lee JY, Oh JM, Baek SC, Leem HH, Park D, Cho ML, Kim H. Potent inhibition of acetylcholinesterase by sargachromanol I from Sargassum siliquastrum and by selected natural compounds. *Bioorg Chem* 2019,89,103043.